High Temperature Insulation Materials for DC Cable Insulation — Part II: Partial Discharge Behavior at Elevated Altitudes

Tohid Shahsavarian, Chuanyang Li, Mohamadreza Arab Baferani, JoAnne Ronzello and Yang Cao

Electrical and Computer Engineering, University of Connecticut, 371 Fairfield Way, Storrs, CT 06269, USA

Xin Wu

United Technologies Research Center, Raytheon Technologies, East Hartford, CT 06108, USA

Di Zhang

Naval Postgraduate School, Monterey, CA 93943, USA

ABSTRACT

Utilizing hybrid electric propulsion systems in the next generation of aircrafts with elevated DC voltage level has raised the concern about the degradation of insulation subjected to partial discharge at high altitude and harsh environment. In this work, the surface discharge behavior of commonly used high-temperature insulation materials in aviation systems (FEP, ETFE, and PEEK) under positive and negative DC and ramp voltage was studied, including the pulse waveform, frequency spectrum, PD count and magnitude. Pressure changes as a significant factor influencing surface discharge phenomenon was thoroughly studied. Dust figure technique was employed after voltage ramping tests for both positive and negative polarities at low pressure to investigate the surface charge accumulation and surface discharge traces, and unveil the involved physical mechanisms at different stages of streamer propagation. The content of this paper provides a reference for surface discharge studies and evaluation of high temperature materials for medium voltage direct current power distribution in the future aviation systems.

Index Terms — aviation system, more electric aircraft (MEA), surface discharge, high-temperature insulation material, dust pattern, DC voltage, partial discharge

1 INTRODUCTION

INCREASE of DC bus voltage and hence power rating for future More Electric Aircraft has brought up concerns of insulating materials degradation owing to the partial discharge (PD) occurrence especially under harsh conditions. In contrast to AC voltage, the nature of numerous discrete physical processes involved in surface and bulk discharges under DC voltage, mostly at microscopic scale, which include the space charge accumulation in the bulk and interfaces, polarization, charge carrier drift and hopping, increases significantly the complexity of partial discharge analysis [1, 2]. Besides, since the conductivity of the intact polymeric insulation is extremely low which strongly depends on the electric field and the temperature, partial discharge pulses under DC voltage typically are of very low repetition rate and low magnitude

which can only be studied with accurate PD acquisition systems over a long duration. This raises the concern about the reliability of PD test circuit and system immunity from environment and circuit noises. On the other hand, the environmental factors such as temperature, humidity and pressure, all represent key influencing factors on surface and creepage discharges, as they could affect photoionization from charge transport and trapping, and ionization of gas molecules in vicinity of gas-solid interface [3].

High-performance and high-temperature polymer insulations are widely used in wires and cables in aircrafts [4–6] to protect them from localized high temperature degradation and electrical fires due to PDs and flashovers, while imparting also good thermal, mechanical and dielectric stabilities [5]; however, their DC characteristics have not been fully studied and understood. The aim of this paper is to investigate the DC partial discharge characteristics of major high-temperature insulation materials under pressure changes

and low pressure operation to provide insights into their DC withstands for manufacturers and designers.

Although there is no widely accepted standard for PD analysis at DC voltage, researchers have discussed several techniques in recent works regarding the detection, representation and analyzation of PD pulses. Morshuis studied the mechanisms of PD under DC voltage and summarized techniques for measuring and analyzing PD patterns [7]. Other PD testing methods under applied DC voltage have been introduced in [8–10]. Also, the impact of pressure on partial discharge behavior in DC voltage has been addressed in a few works [10–16], but complete study has not been carried out, especially on high-temperature insulation materials. Moreover, the characteristic of partial discharges along the insulating surface has only been studied using sphere/needle-plane configuration under AC or positive and negative ramp voltages with variable rate of rise (0.05 to 1 kV/s) [17, 18].

In this paper, the surface discharge, frequently reported as the key deteriorating factor of insulation materials used in aerospace power distribution system, has been systematically studied. A new technique to study the impact of pressure variation during takeoff and landing has been proposed. Three sets of tests for evaluating the impact of pressure on surface discharge behavior under fixed positive and negative DC voltages, ramp voltage at ambient and low pressure atmosphere, as well as surface charge accumulation and discharge trace using the dust figure technique have been carried out and discussed.

2 EXPERIMENTAL 2.1 TEST SETUP

The PD test circuit was adopted based on standard AC PD measuring test (IEC60270) including power supply (50kV), coupling capacitor (1nF), measuring impedance (LDM-5) connected to data acquisition system, along with the diode and smoothing capacitor set (90.4 nF) for rectification, and the vacuum chamber (Figure 1). It has been reported that this capacitive circuit can be used for both AC and DC PD tests without extra modification [4] although more accurate data

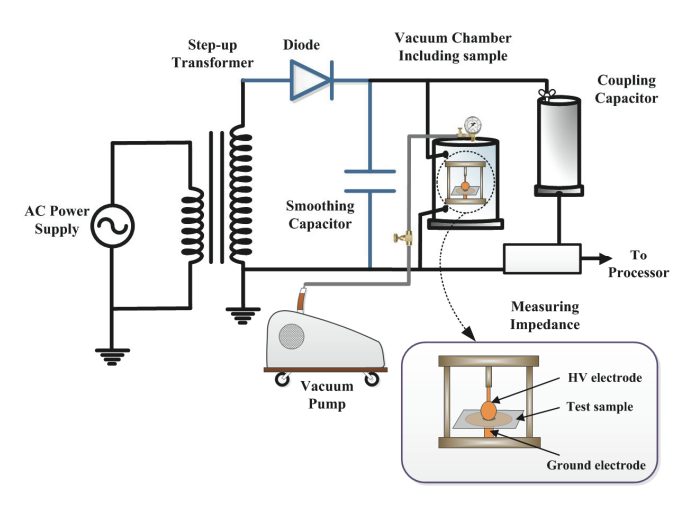


Figure 1. PD test setup.

processing algorithm with higher precision and special noise rejection algorithm is required in order to detect discharge pulses with low magnitude and wide range of frequency content at DC voltage.

In this work, three types of commonly used, commercially available high-temperature insulation films, FEP, ETFE and PEEK have been procured from Goodfellow. Thickness of all the samples are 240 µm. It is noteworthy that in each set of PD tests, virgin samples have been used in order to avoid impact of polarization and space charge accumulation from previous tests. Also, one side of the films was sputter coated with gold/palladium (Au/Pd, 80/20) to ensure good contact between film and ground electrode for dust figure inspection which will be explained in Section 2.2.

As shown in Figure 1, sphere-plate configuration was used, with brass electrodes with diameters of 12.5 mm and 5 cm, respectively. This electrode configuration was chosen to generate sufficiently high electric field to ignite the surface discharge but without impairing the surface in the case of arcing at low pressure.

2.2 TEST PROCEDURE

For pressure variation test, a mechanical vacuum pump was connected to the test chamber and the pumping can be regulated to decrease and increase the pressure smoothly between 100 kPa, the ambient pressure, and 20 kPa, which corresponds to the pressure level at altitudes around 35000–40000 feet where commercial airplanes fly. Fitted pressure rising and dropping curves from measured pressure data have been plotted in Figure 2. The repeatability of the pressure variation operation was confirmed with recorded pressure data over many runs.

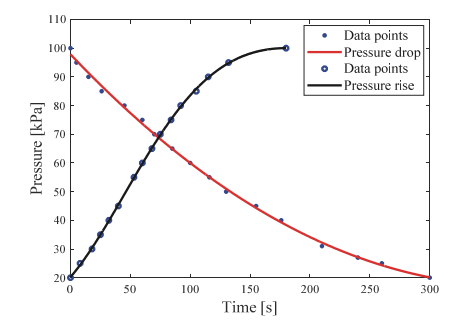


Figure 2. Fitted curves of pressure variation in each voltage level.

A simple electrostatic model was developed in COMSOL to estimate roughly the electric field intensity for this electrode configuration. Each complete test was carried out at three voltage levels (V_{1,2,3}=2, 4, and 6 kV, respectively), of which, the corresponding electric field maximum and normal across the sample are roughly 16, 32, 48 kV/mm, and 8, 16, and 24 kV/mm, respectively. Same test procedure of three voltage steps has been conducted for positive and negative polarities using virgin samples cleaned up with ethanol, as depicted in Figure 3. In each 5 minutes time interval, PD signal has been monitored and acquired. Some authors have suggested to do PD tests at DC voltage for more than 30 mins to evaluate consistency of PD occurrence in ambient condition [8];

however, there is no universally accepted standard for PD test at DC voltage.

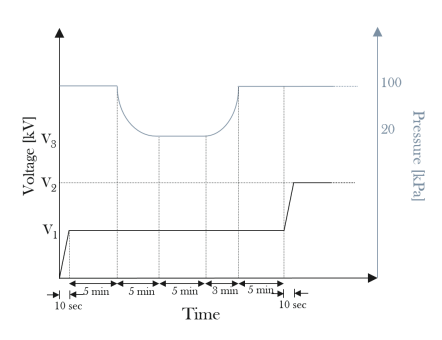


Figure 3. Pressure change test at three voltage levels.

In addition, in order to evaluate the propagation of surface discharge over the samples, two other sets of tests were carried out:

- PD tests for positive and negative ramp voltage at ambient pressure and 20 kPa: The positive and negative ramp voltage was applied up to 6 kV with the rate of 200 V/s (within 30 seconds) on virgin samples, and PD data were acquired for 40 seconds from the beginning of test.
- 2) Surface charge distribution study after applying ramp voltage up to ±6kV based on dust patterns.

For dust pattern study, the positive and negative ramp voltages were applied on the surface of new samples included inside the chamber under low pressure (20 kPa). In order to obtain surface charge distribution pattern after the test, the natural dust was sifted and fine particles were dried inside an oven for half an hour at 120°C. Then, fine dust particles were sprinkled near the inclined film samples against the mild wind flow. The formed pattern known as the dust pattern can represent surface charge accumulation and surface discharge path over the film samples.

2.3 DATA ACQUISITION AND POST-PROCESS

The PD measurement was performed using TechImp PD baseII acquisition unit with a high sampling rate (200 MS/s) and wide bandwidth (16–48 MHz). PD data including magnitude, time interval to the previous pulse, pulse waveforms are extracted from the acquisition system. MATLAB was used for post-processing all the waveforms to separate the detected noises from the real PD pulses and extract PD pulse waveforms. Any PD pulse above 20 pC is triggered by processor as measured real PD. This pulse magnitude, which is higher than the suggested amplitude by IEC 60270, was chosen to account for the wide frequency acquisition capability of our instrument (16 kHz-48 MHz) with respect to IEC standard bandwidth (115-440 kHz), as the former is more sensitive in picking up external noises and unwanted discharges inside the chamber especially for tests performed at low pressure.

All tests have been carried out three times, during which similar trends were observed; however, slight variance of no more than 15% could be observed between the recorded PD numbers in these test runs. Also, creepage discharges were observed with magnitudes higher than 3 V which were discarded after extraction of recorded data from PD processor. MATLAB code was adopted for adjusting time interval between PDs after monitoring all PDs and discarding any significant noise pulses and creepage discharges. Since all PD tests have been done inside an EMI shielded room, white noises having the magnitudes lower than 20 pC do not affect the PD results. All PD magnitudes lower than 3 V have been extracted and presented in the next sections.

Figure 4 shows examples of detected PD pulses for ETFE sample during the pressure change under applied positive and negative DC voltages. The same magnitude of pulses has been chosen to be conducive in comparing the PD waveforms.

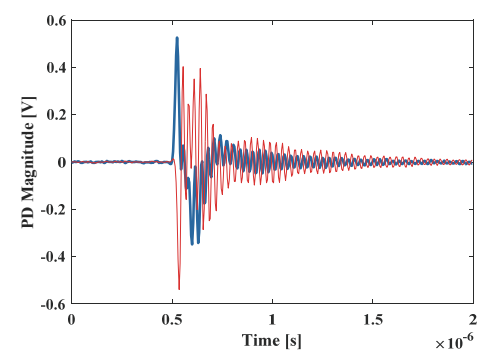


Figure 4. PD pulses detected at positive and negative polarities with the same selected magnitude.

In addition to the PD magnitudes and time intervals between PDs, frequency spectra of all PD waveforms were extracted. The equivalent time-length and equivalent bandwidth of each single detected pulses are calculated per Equations (1)–(3) to compare time and frequency information of PDs in separate mapping plots [19]:

$$t_0 = \frac{\sum_{i=0}^{K} t_i \cdot s_i(t_i)^2}{\sum_{i=0}^{K} s_i(t_i)^2}$$
 (1)

$$T^{2} = \frac{\sum_{i=0}^{K} (t_{i} - t_{0})^{2} \cdot s_{i}(t_{i})^{2}}{\sum_{i=0}^{K} s_{i}(t_{i})^{2}}$$
(2)

$$W^{2} = \frac{\sum_{i=0}^{K} f_{i}^{2} |X_{i}(f_{i})|^{2}}{\sum_{i=0}^{K} |X_{i}(f_{i})|^{2}}$$
(3)

where T^2 and W^2 are equivalent time-length and equivalent bandwidth which are calculated using K sampled single PD pulse signal $s_i(t_i)$, and time-barycentre t_0 , and frequency component of signal $X_i(f_i)$. T-F mapping is generally used for PD source classification and clustering.

3 RESULTS

3.1 PD RESULTS FOR PRESSURE CYCLING TEST

Pressure change test was carried out for each virgin sample at each voltage level continuously stepped up to 2, 4, and 6 kV as depicted in Figure 3. This pressure changing trend was chosen to emulate taking-off and landing modes of aviation

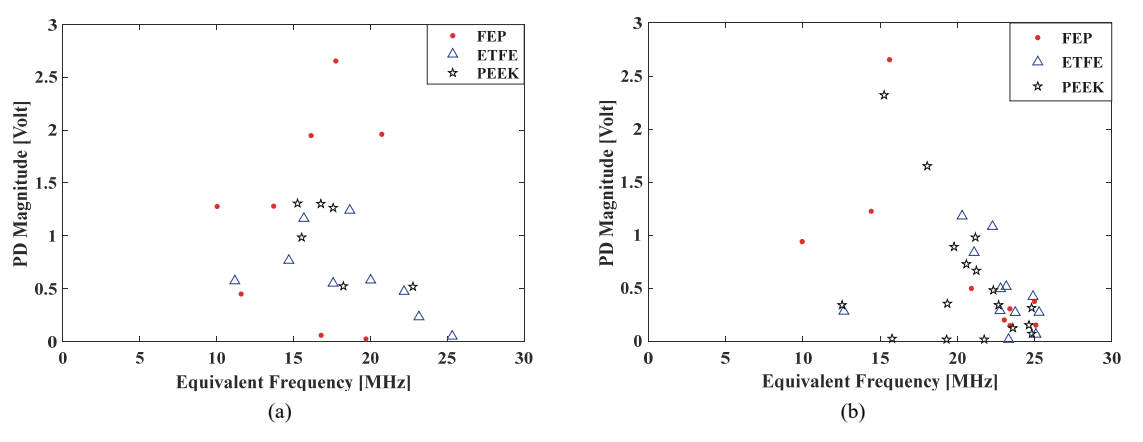


Figure 5. T-F mapping of recorded PDs during decreasing the pressure at 4 kV: (a) positive and (b) negative polarities.

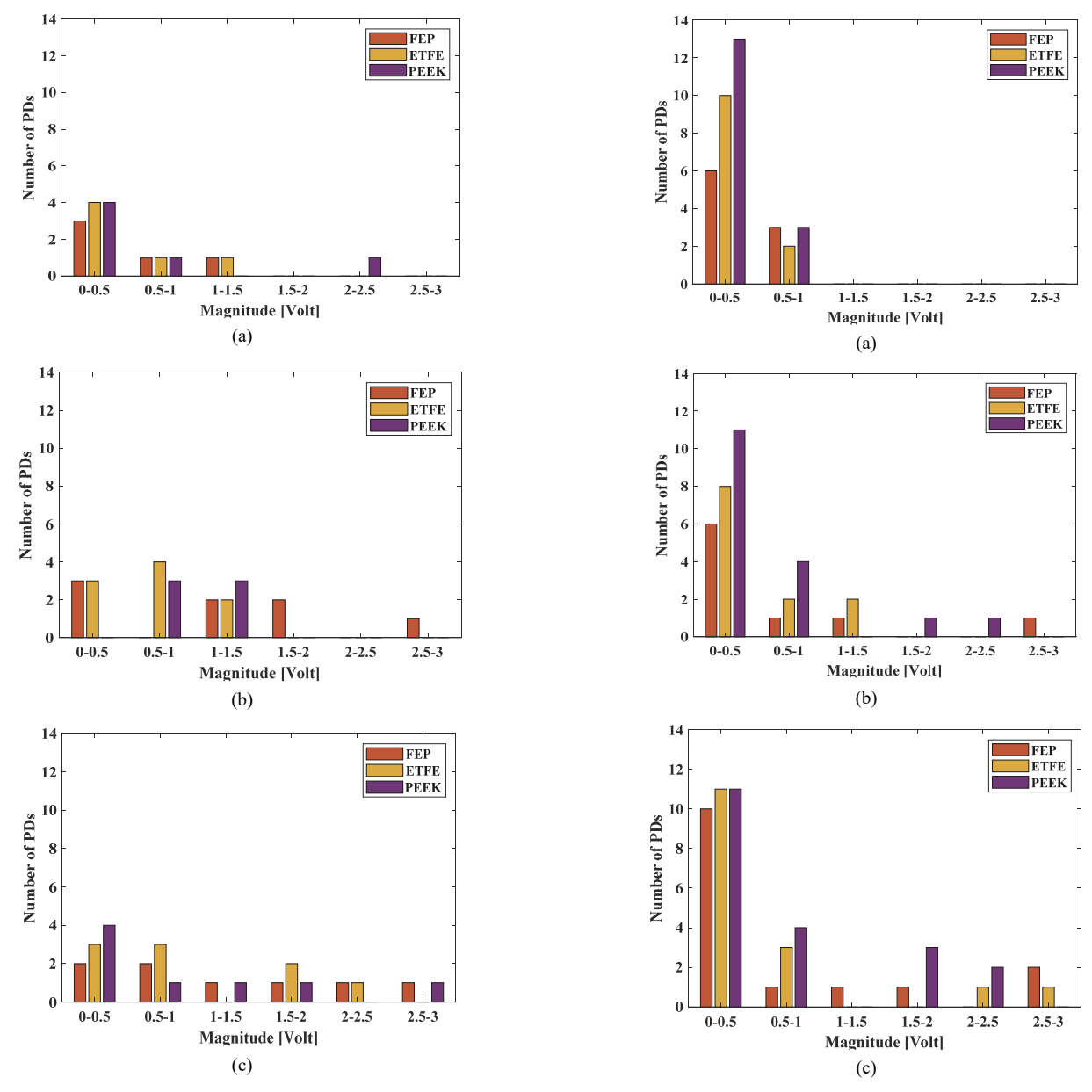


Figure 6. Categorized PD pulses during decreasing the pressure based on magnitude at: (a) +2 kV, (b) +4 kV, and (c) +6 kV.

Figure 7. Categorized PD pulses during decreasing the pressure based on magnitude at: (a) -2 kV, (b) -4 kV, and (c) -6 kV.

systems. Test shows PD occurs once pressure drops and magnitude of PDs increases at lower pressure levels; however, it stops when pressure settles at its lowest level studied in this work (20 kPa). Therefore, no PD was detected for pressure increase and at stable pressure level in aforementioned sensitivity level, and extracted PD results during decrease of pressure are discussed in this section. Figure 5 shows equivalent frequency information of PD pulses with corresponding magnitude for recorded PD pulses during decrease of pressure at 4 kV for both polarities. Similar patterns were shown for applied 2 and 6 kV. As can be seen, frequency contents of all detected PDs are in the range of 10 to 25 MHz.

Figures 6 and 7 show the number of detected PDs based on categorized PD magnitudes for test samples under positive and negative polarities, respectively. Majority of detected pulses at ±2kV are lower than 1V. Higher PD magnitudes occur at 4 and 6 kV for both polarities. Number of PDs at negative polarity for all three voltage levels is higher than positive polarity. Unlike negative polarity, PD magnitude of pulses at 4 kV is less than 2 V. Wide range of PD magnitudes are detected for both positive and negative polarities at 6 kV.

3.2 PD RESULTS FOR RAMP VOLTAGE TEST

Test was carried out to investigate the impact of ramp voltage on surface discharge propagation over the hightemperature insulation materials. Figures 8 and 9 show the magnitude of detected PDs for ±6kV during the test period of 40 seconds. As can be seen in these figures, discharges at ambient pressure start to occur after 10 and 17 seconds for positive and negative polarities which correspond respectively to voltages of +2kV and -3.5kV. In addition, distribution of PDs for negative polarity is denser than positive polarity which implies higher cumulative PD charges involved in discharge process at positive polarity with respect to negative polarity. The same observation can be noticed for the test at 20 kPa which shows wide ranges of PD magnitudes during voltage ramping for positive polarity with respect to negative polarity. More details of extracted results from these figures, i.e., number of detected PDs, average of PD magnitudes, and total PD charges, are presented in Section 4. Overall, it can be concluded that, at ambient pressure, electric field with high intensity generates PD pulses with higher magnitude. Even though the probability of PD under positive polarity is lower than negative polarity because of less contribution of positive ions in the discharge process, these PDs have respectively higher magnitude since time interval between PDs is slightly higher at both ambient and low pressure. However, discharges at lower pressure have higher repetition rate and magnitude, because hopping and transport of electrons and ions at the interface of surface layer and high conductive atmosphere (low pressure) is significantly easier with respect to the ambient pressure.

3.3 DUST FIGURE

Focus of this test is to show impact of polarity on discharge pattern and to compare the discharge area for these high temperature insulation materials at 20 kPa. Figure 10 shows

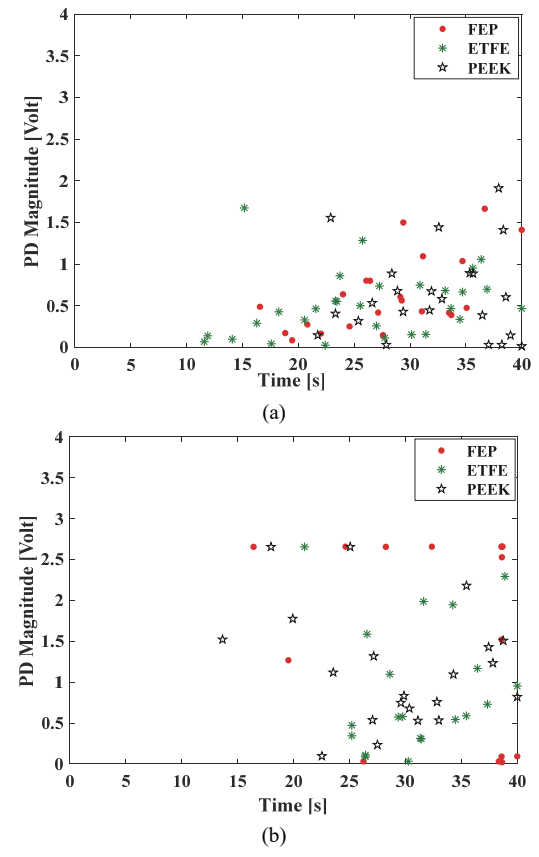


Figure 8. PD magnitude of detected pulses during ramping the voltage up to 6 kV at: (a) ambient pressure, and (b) 20 kPa.

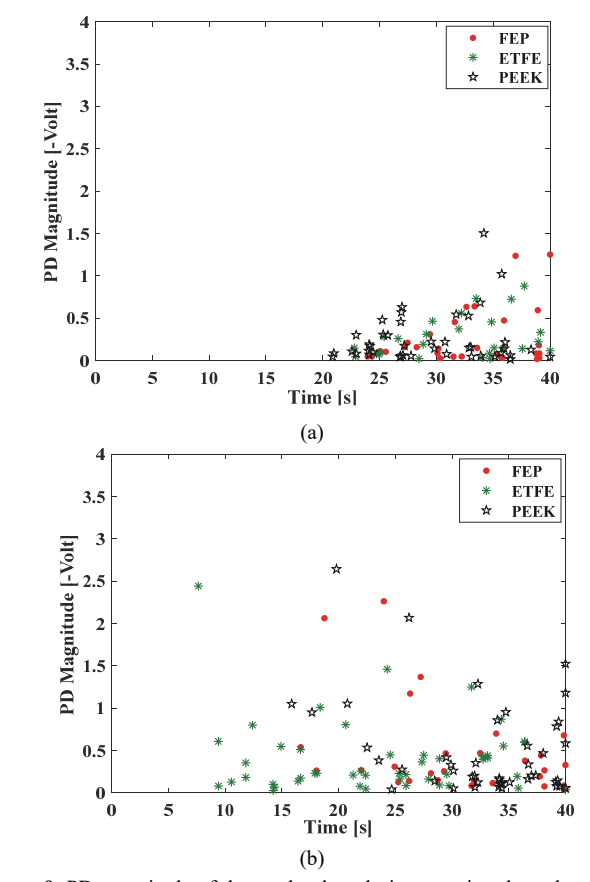


Figure 9. PD magnitude of detected pulses during ramping the voltage up to -6 kV at: (a) ambient pressure, and (b) 20 kPa.

these dust figure patterns for both polarities, when the voltage was ramped for both up to 2 kV. The area of discharge at negative polarity is noticeably bigger than at positive polarity for all samples. At this voltage level, majority of surface discharges in positive polarity are concentrated in the center of positively charged area where high voltage sphere was attached to the surface. This area shows accumulated homocharges on the surface and becomes bigger at applied higher voltages. In contrast, negative streamer discharges at negative polarity of voltage proceed outwards which suggests transport of electrons on the surface along the discharge trace. As long as these discharges have not occurred and elongated beyond the accumulated charge area, surface charge area for all samples is almost the same.

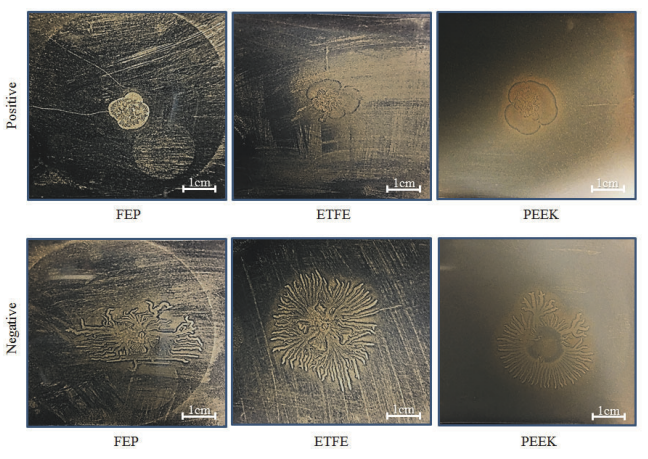


Figure 10. Dust figures formed on the surface of test samples after increasing the voltage up to ± 2 kV at 20 kPa.

The same trend can be seen in Figure 11 for ramp voltage up to 6 kV, i.e., concentrated pattern in the center of positively charged area vs streamer alike outward discharge at negative polarity, with generally bigger accumulated charge and surface discharge area. Although the discharge patterns for positive and negative voltages are different, covered accumulated charge and discharge areas in these dust patterns, depending on applied voltage magnitude, are nearly the same for all three samples.

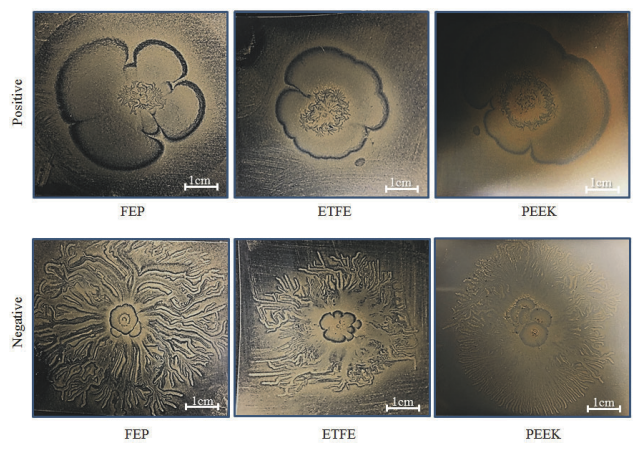


Figure 11. Dust figures formed on the surface of test samples after increasing the voltage up to ± 6 kV at 20 kPa.

4 DISCUSSION

4.1 SURFACE DISCHARGE MECHANISM

Several physical processes are involved in the initiation and development of surface discharge. Its initiation can be due to field electron emission from the cathode triple junction (CTJ) for the classical electrode contact. The secondary electron emission (SEE) can occur due to bombardment of emitted electrons on insulator surface. It is expected that under lower electric field, charge carriers are injected into the surface of insulating material rather than emitting into the vacuum when they obtain the energy higher than work function of electrode metal [20]. After relaxation of electric field in vicinity of electrodes by injected charges, local electric field around the charged area will be increased which can provide enough energy for charges to proceed outwards. Through processes like the hopping, these charges can transport along the surface layer. The electroluminescence (EL) phenomena occurs afterwards owing to the radiative recombination of electrons and holes [21]. In positive polarity, injected positive ions have low mobility and less likely to participate in discharge process at low electric field which is the reason that centralized injected homocharges for applied positive polarity of 2 and 6 kV over the surface of the samples can be seen in dust patterns in Figures 10 and 11. The development of streamer discharge is more obvious in dust patterns related to negative polarity under which high density of electrons with higher velocity can transport along the applied tangential electric field over the surface.

4.2 PRESSURE DEPENDENCE OF SURFACE DISCHARGES

Based on the results presented in Figures 6 and 7, number of detected PDs (n), average of PD magnitudes (\bar{Q}), and total PD charges $(Q_T = \sum_{i=1}^n Q_i)$ have been extracted and given in Table 1. Total PD charges can be an effective parameter for comparing the results. As can be seen, the total PD charge is much lower for test results obtained at ±2 kV than at ±4 and ±6 kV for all samples. Although streamer mechanism for negative and positive polarities are different and discharge process can comprise different stages as explained in section 4.4, number of PD pulses at negative polarity is generally higher than positive polarity. On the flip side, positive PD charge average is generally higher than negative PD charge average for all samples. Considering the total PD charge values for both polarities in this test, FEP and ETFE have highest and lowest surface discharge intensity, respectively. As mentioned in part I [22], FEP has highest charge density on the electrode-dielectric interface among the samples. ETFE has higher charge density in interface than PEEK but charge accumulation process in ETFE takes longer than PD testing time. PD results imply direct relationship between charge density in the interface and discharge intensity. However, further investigation should be conducted to verify this relationship.

The voltage ramping test was carried out to investigate the impact of polarity and pressure on streamer discharge as well

Voltage level	FEP				ETFE		PEEK		
[kV]	n	$ar{Q}$	Q_T	n	$ar{Q}$	Q_T	n	$ar{Q}$	Q_T
+2	5	0.38	1.92	6	0.37	2.21	6	0.68	4.09
+4	8	1.21	9.65	9	0.62	5.62	6	0.98	5.90
+6	8	1.25	9.98	9	0.96	8.64	8	0.79	6.30
-2	9	-0.39	-3.51	12	-0.23	-2.79	16	-0.29	-4.67
-4	9	-0.72	-6.50	12	-0.47	-5.69	17	-0.55	-9.36
-6	15	-0.73	-10.99	16	-0.50	-7.95	20	-0.71	-14.19

 Table 1. Detailed extracted PD data during pressure drop at different voltage and polarities corresponding to Figures 6 and 7.

Table 2. Extracted PD data during voltage ramp up to 6kV for both polarities corresponding to Figures 8 and 9.

Voltage ramp	Pressure	FEP				ETFE			PEEK		
		n	$ar{Q}$	Q_T	n	$ar{Q}$	Q_T	n	$ar{Q}$	Q_T	
0 to +6 kV	100 kPa	22	0.63	13.83	29	0.51	14.80	23	0.63	14.45	
0 to +6 kV	20 kPa	15	1.61	24.16	20	0.92	18.35	21	1.15	24.23	
0 to -6 kV	100 kPa	30	-0.25	-7.55	26	-0.27	-6.91	42	-0.25	-10.44	
0 to -6 kV	20 kPa	28	-0.48	-13.56	48	-0.4	-19.40	46	-0.49	-22.40	

as surface interaction of insulating materials for applied ramp voltage. The constant ramping rate of 0.2 kV/s has been considered for ramping voltage up to 6kV in both polarities under ambient pressure and 20kPa. The same abovementioned PD parameters have been obtained for this test and given in Table 2. As can be seen, the number of PDs generally is higher for negative polarity with respect to positive polarity of applied voltage.

However, average of PD magnitudes for positive polarity is much higher than negative polarity. Comparing the total PD charge of positive and negative polarities by multiplying number and average charge of PDs could not serve as useful parameters. The reason is that the mechanisms of surface discharge for positive and negative polarities are different and comparing total charges contributed to streamer discharge is not meaningful. However, the total PD charges calculated for tests at ambient and low pressure (20 kPa) can be separately compared for applied positive and negative polarity. This value is higher at low pressure than ambient pressure as expected. However, it is worth noting that the total PD charges during ramping up the voltage in low pressure comparing to ambient pressure is much higher in negative polarity with respect to positive polarity.

Overall, PEEK at negative polarity and FEP at positive polarity have higher total PD charge. Bigger area of dust pattern formed at low pressure for positive polarity shown in Figure 11 (obtained in separate tests) corresponds with total PD charge values. FEP and PEEK having almost the same total positive PD charge (~24 volts) have the same accumulated surface charge at 20 kPa. ETFE has slightly smaller area and smaller total PD charge. For positive and negative polarities at 20 kPa, all samples have significantly higher discharge area and higher average and total PD magnitude as presented in Table 2. Also, dust pattern for FEP shows more intense discharge area which is due to occurred and recorded creepage discharge. This type of discharge with bigger PD magnitude was not detected during separate ramping test purposely carried out for this part of the

experiment. The aim was to conduct more tests at the same condition and assess the correlation between dust pattern and measured PD results.

4.3 SURFACE CHARGE AND PD PROPAGATION BASED ON DUST FIGURE TEST

As explained in [23], at positive polarity of applied voltage, free electrons move toward the positive electrode. On the other hand, positive ions are injected into the surface and accumulate around the electrode. Electrons collide with the neutral molecules and, due to the ionization process, more electrons and positive ions are generated. Small discharge traces in the center of accumulated charges for dust patterns belonging to positive polarity at low voltage can be due to this process intensified by voltage ramping up. Positive ions move in the opposite side and in turn electric field around positively charged area increases and another set of discharges occur in outside of charged area at higher electric fields as can be seen in Figure 11 for positive polarity. Discharge process on the surface is stopped when the electric field on the streamer tip is not sufficient to ionize the molecules [24].

For negative polarity, emitted free electrons can be a contributing factor for streamer discharge on the surface even at lower electric field formed at -2 kV applied. Traces of electron drifting away from the high voltage electrode in the process of surface discharge can be seen in Figures 10 and 11 for patterns belonging to negative polarity of applied voltage. Wider branches observed in the patterns of negative polarity belong to surface discharges with bigger magnitudes which are attributable to transport of higher number of electrons in the discharge process.

5 CONCLUSIONS

In this paper, performance of high-temperature insulation materials intended for DC cabling and power distribution system for future aviation systems subjected to high altitude has been investigated. Test results show that during taking-off mode under which insulation is subjected to lower pressure, the surface discharge can be initiated with higher magnitudes. Meanwhile, accumulated surface charge can have significant impact on further discharge propagation depending on charge polarity. At positive polarity, positively charged area is dominant with discharge traces adjacent to high voltage electrode (sphere) with high electric field intensity; while, at negative polarity, presence of negative charges with high mobility facilitates discharge progression which was clearly observed in dust patterns. Extracted parameters from recorded PD test data (PD count, average and total PD charge) demonstrate difference in the discharge intensity among the materials which can be attributable to insulation properties such as electrical conductivity and permittivity. However, micro-scale study will be required to identify main cause of these differences in future studies.

Some of the main outcomes of test results can be concluded as follows:

- (1) Number of detected PD pulses in negative polarity is higher than positive polarity; however, average PD magnitude for positive polarity is relatively higher than negative polarity. So, it suggests that the PD test at positive and negative polarity shall be studied separately in future research works.
- (2) Total PD charge at low pressure is higher than at ambient pressure. This difference is higher for negative polarity with respect to positive polarity.
- (3) Results obtained for FEP and PEEK show more intense surface discharge based on pressure drop and voltage ramping tests as well as dust pattern observations. In authors' future work, accurate investigation for evaluating the intensity of surface discharge will be conducted by considering the impact of polarity on discharge propagation along with surface discharge modeling.
- (4) Total PD charge values for ramp voltage test can be related to concentrated dust areas. This comparison is more obvious for applied positive voltage where dust figures have not covered all the surface of samples, although the obtained total PD charges from the PD tests show clearly higher values at low pressure corresponding to bigger discharge and accumulated charge area in dust patterns.

ACKNOWLEDGMENT

The authors would like to thank NASA, United Technology Research Center (UTRC) and NSF (1650544) for funding support.

REFERENCES

- G. Thomas, et al, "Interim Report of WG D1.63: Progress on Partial discharge detection under DC voltage stress", CIGRE, 2019.
- C. Y. Li et al, "Charge cluster triggers unpredictable insulation surface flashover in pressurized SF6," J. Phys. D: Appl. Phys., doi.org/10.1088/ 1361-6463/abb38f, 2020.
- [3] C. Li et al, "Surface charge migration and dc surface flashover of surface-modified epoxy-based insulators," J. Phys. D: Appl. Phys., vol. 50, p. 065301, 2017.
- M. Tooley and D. Wyatt, Aircraft electrical and electronic systems: principles, operation and maintenance, Elsevier, Amsterdam, The Netherlands, 2009.

- [5] J. Kurek et al, Aircraft wiring degradation study, US Department of Transportation, Federal Aviation Administration, Report No. DOT/FAA/ AR-08/2, 2008.
- R. Domingo, Aviation maintenance technician handbook-Airframe, US Department of Transportation, Federal Aviation Administration, Flight Standards Service, Vol. 1, 2018.
- P. H. F. Morshuis and J. J. Smit, "Partial discharges at DC voltage: their mechanism, detection and analysis," IEEE Trans. Dielectr. Electr. Insul., vol. 12, pp. 328-340, 2005.
- A. Pirker and U. Schichler, "Partial discharge measurement at DC voltage — Evaluation and characterization by NoDi pattern," IEEE Trans. Dielectr. Electr. Insul., vol. 25, pp. 883–891, 2018.
- P. Trnka, J. Hornak, M. Svoboda, and J. Pihera, "Partial discharges under DC voltage in paper-oil insulating system," IEEE Int. Conf. Prop. Appl. Dielectr. Mat. (ICPADM), 2015, pp. 436-439.
- [10] P. Romano, G. Presti, A. Imburgia, and R. Candela, "A new approach to partial discharge detection under DC voltage," IEEE Electr, Insul. Mag., vol. 34, no. 4, pp. 32-41, 2018.
- [11] I. Cotton et al, "Design considerations for higher electrical power system voltages in aerospace vehicles," IEEE Int. Power Mod.High Voltage Conf. (IPMHVC), 2016, pp. 57-61.
- [12] X. Liu, D. G. Kasten, and S. A. Sebo, "Partial discharge measurements for a twisted pair of insulated conductors at low pressures in air, argon and helium," IEEE Int. Symp. Electr. Insul. (ISEI), 2006, pp. 286-289.
- [13] D. Kasten et al, "Flashover and breakdown investigations of aircraft wiring in low pressure environment," IEEE Int. Power Mod. High Voltage Conf. 2010, pp. 501-504.
- [14] E. Husain and R. S. Nema, "Surface Discharge Studies with Uniform Field Electrodes at Low Pressures," IEEE Trans. Electr. Insul., vol. EI-16, pp. 128-133, 1981.
- [15] A.Sobota et al, "Speed of streamers in argon over a flat surface of a dielectric", J. Phys. D: Appl. Phys., vol. 42, p. 015211, 2019.
- [16] M. Akyuz et al, "Positive streamer discharges along insulating surfaces," IEEE Trans. Dielectr. Electr. Insul., vol. 8, pp. 902-910, 2001.
- [17] H. Mu et al, "Investigation of surface discharges on different polymeric materials under HVAC in atmospheric air," IEEE Trans. Dielectr. Electr. Insul., vol. 18, pp. 485-494, 2011.
- [18] N. C. Mavrikakis and P. N. Mikropoulos, "Negative Corona Characteristics on RTV SIR Coated Glass Insulating Surface under Ramp High Voltages," IEEE Int. Conf. High Voltage Eng, Appl., 2018,
- [19] A. Contin et al, "Digital detection and fuzzy classification of partial discharge signals," IEEE Trans. Dielectr. Electr. Insul., vol. 9, pp. 335-348, 2002.
- [20] G. J. Zhang et al, "Optical studies of surface discharge under DC voltage in vacuum," IEEE Int. Symp. Discharges Electr. Insul. Vac.(ISDEIV), 2000, vol. 1, pp. 112-115.
- [21] C. Li et al, "Fluorine gas treatment improves surface degradation inhibiting property of alumina- filled epoxy composite," AIP advances, vol. 6, pp. 025017-1-6, 2016.
- M. Arab Baferani et al, "High temperature insulation materials for DC cable insulation-Part I: Space charge and conduction," IEEE Trans. Dielectr. Electr. Insul., accepted.
- [23] M. Pantelis and S. Pavlos, "Investigation of the Partial Discharge Characteristics on PTFE and PMMA Surfaces Under Positive Ramp High Voltages with Variable Rate of Rise," IEEE Int. Symp. High Voltage Eng., 2019, pp. 1133-1145.
- T. N. Tran, "Surface discharge dynamics: Theory, Experiment and Simulation," Ph.D. Thesis, University of Southampton, 2010.



Tohid Shahsavarian received his B.Sc. degree in electrical engineering from the University of Tabriz in 2011, and the M.Sc. degree from University of Science and Technology, Iran, in 2013. Then, he worked in the Department of Transmission and Distribution in Monenco Iran Consulting Engineers Company. He is currently working toward his Ph.D. degree in electrical engineering at University of Connecticut. His research interests include partial discharge analysis and risk

assessment of AC and DC power cables, reliability analysis of HVDC grids, and geomagnetic disturbances.



Chuanyang Li received his Ph.D degree in the Department of Electrical Engineering, Tsinghua University in 2018. He worked as a Postdoctoral Fellow at the Department of Electrical, Electronic and Information Engineering "Guglielmo Marconi" of the University of Bologna, Italy from 2018 to 2019. Currently, he is with the Department of Electrical and Computer Engineering & Institute of Materials Science, University of Connecticut, as a Postdoctoral Fellow. His research interests include

surface charge behavior and modification methods and PD properties of high temperature material in harsh conditions. He served as the Lead Guest Editor of the IEEE Trans. Dielectr. Electr. Insul. Special Issue on Advanced Dielectrics for Gas-Insulated Transmission Lines in 2018; NanoTechnology Focus Collection on Focus on Gas-Solid Interface Charging Physics in 2020, and the Guest Editor in High Voltage Special Issue on Interface Charging Phenomena for Dielectric Materials. He is an associate editor of IET High Voltage. He can be reached at lichuanyangsuper@163.com.



Mohamadreza Arab Baferani received the BSc degree in electrical engineering from the Iran University of Science and Technology, Iran and MSc from University of Tehran, Iran. Currently, he is a PhD student in electrical engineering and research assistant in University of Connecticut. His main research interests are high voltage engineering and HVDC cable systems.



JoAnne Ronzello is a research specialist at the Institute of Materials Science/Electrical Insulation Research Center at the University of Connecticut. JoAnne has spent more than 35 years working in the area of dielectrics including high voltage testing, failure analysis, dielectric spectroscopy, and novel experimental development. She holds undergraduate degrees in chemistry and electrical engineering.



Yang Cao graduated with B.S. and M.S. in physics from Tongji University in Shanghai, China, and received his PhD from the University of Connecticut in 2002, after which he served as a senior electrical engineer at GE Global Research Center until 2013. He is currently a full professor at the Electrical and Computer Engineering of the University of Connecticut. Dr. Cao is also the Director of the Electrical Insulation Research Center, Institute of Materials Science and the Site Director of the NSF

iUCRC Center on High Voltage/Temperature Materials & Structures. His research interests are in the physics of materials under extremely high field and the development of new dielectric materials, particularly the polymeric nanostructured materials, for energy efficient power conversion and renewables integrations, as well as for novel medical diagnostic imaging devices.